Food Analytical Methods
https://doi.org/10.1007/s12161-024-02606-9

RESEARCH

A Novel Stability-Indicating RP-HPLC Method for the Simultaneous Estimation and In Vitro and In vivo Evaluation: Curcumin and Naringin Co-amorphous System

Pooja Mallya[1] · Dani Lakshman Yarlagadda[2] · Shaila Lewis[1]

Received: 20 July 2023 / Accepted: 26 February 2024

Abstract
Curcumin (CUR) is a phytochemical widely used in food industries, cosmetics, and in the treatment of various ailments. It is a polyphenol derived from turmeric and is often considered the golden spice. CUR has a low solubility of less than 1 µg/ml and poor oral bioavailability which can be improved by co-amorphization with naringin (NRG). Analytical method to simultaneously quantify CUR and NRG is not reported in literature. This study aimed to develop a stability-indicating reverse phase HPLC method in gradient mode to simultaneously quantify CUR and NRG in co-amorphous system. The co-amorphous system of CUR and NRG in molar ratios 1:1 and 1:2 was prepared by quench cooling technique. The separation was attained on a Genesis C18, (4.6 mm × 150 mm, 4 µm) column with the mobile phase comprising of methanol and a 0.1% acetate buffer pH 3.8 at a single wavelength, 289 nm. CUR and NRG eluted at 5.1 and 11.1 min, respectively. For both the molecules, the linearity range was 0.125–16 µg/ml with LOD and LOQ of 0.063 and 0.125 µg/ml. The method developed was validated as per International Conference on Harmonization (ICH) guidelines for linearity, accuracy, precision, and robustness. The method was used to estimate CUR and NRG content in co-amorphous mixture and for in vitro evaluation.

Keywords Co-amorphous mixture · Curcumin · Naringin · High performance liquid chromatography · Method validation · Stability indicating

Introduction

Phytoconstituents represent a huge group of therapeutically active compounds applicable to treat variety of diseases in humans (Sayed et al. 2019). Phytoconstituents such as quercetin, myricetin, and other flavonoids have been used in the treatment of neurodegenerative diseases (Singh et al. 2021); curcumin (CUR), quercetin, berberine, silymarin, resveratrol, and capsaicin in inflammatory diseases (Khan et al. 2021; Chen and Liu 2022); CUR, ombuine, indigtone, and anastatin in liver diseases (Ali et al. 2019); D-limonene, epigallocatechin gallate, thymoquinone, beta-lapachone, campothecin, genistein, taxanes, and vinca alkaloids in cancer (Nakonieczna et al. 2020; Asati 2022; Kaur et al. 2022); avarol, vindoline, catharanthine, berberine, and pinolene in diabetes (Alam et al. 2022; Behl et al. 2022); CUR, naringenin, quercetin, mimosine, diosgenin, catechin, and rutin in gynaecological disorders such as polycystic ovary syndrome and endometriosis (Balan et al. 2021; Temkar and Menon 2022; Chorosho et al. 2023; Luo et al. 2023); lycopene and carotene in aging-related diseases (Xue et al. 2021); kaempferol, myricetin, and silybin in infectious diseases (Kancherla et al. 2019; Joshi and Prabhakar 2020; Das et al. 2021); and naringin (NRG), hesperidin, and mangiferin in renal fibrosis (Xu et al. 2021). Albeit of desired therapeutic efficacy, challenges such as low solubility in water, insufficient absorption when taken orally, restricted stability, and a brief duration of action impede the molecules from being successfully introduced into the market (Suresh et al. 2014).

CUR (Fig. 1a) is a widely used phytochemical that is generally recognized as a safe (GRAS) molecule by the United States Food and Drug Administration (USFDA) (Ipar

✉ Shaila Lewis
s.lewis@manipal.edu

[1] Department of Pharmaceutics, Manipal College of Pharmaceutical Sciences, Manipal Academy of Higher Education (MAHE), Manipal 576104, Karnataka, India

[2] Department of Pharmaceutical Quality Assurance, Manipal College of Pharmaceutical Sciences, Manipal Academy of Higher Education (MAHE), Manipal 576104, Karnataka, India

Published online: 09 March 2024

et al. 2019). CUR is a polyphenol derived from turmeric or *Curcuma longa*. CUR is been used as a spice, food additive, natural colouring agent, preservative, and pH-sensitive indicator in food industries (Jiang et al. 2021). It is used in the treatment of cardiovascular disease (Norooznezhad et al. 2020), diabetes (Bulboacă et al. 2019), cancer (Bolat et al. 2020; Mardani et al. 2020), neurodegenerative disorders (Yavarpour-Bali et al. 2019; Lin et al. 2020), polycystic ovary syndrome (Sohaei et al. 2019), and chronic disorders (Ghelani et al. 2019; Tagde et al. 2021). CUR has poor aqueous solubility (< 1 µg/ml) (Liu et al. 2020; Tabanelli et al. 2021) and undergoes P-glycoprotein (P-gp) efflux limiting its membrane permeability, while the poor oral bioavailability of CUR is due to extensive phase II metabolism in the presence of uridine 5′-diphosphate-glucuronosyltransferase (UGT) and β-glucuronidase enzymes (Han et al. 2023; Wdowiak et al. 2023). Strategies to enhance the solubility and oral bioavailability of CUR for better therapeutic effects have been attempted and are continuing with the advances in drug delivery technology (Yildiz et al. 2019).

Recently, co-amorphous systems (CAM) combining two drugs, or drug and excipients, have been employed for solubility enhancement of poorly soluble drugs (Mizoguchi et al. 2019). CAM is the mixture of two or more low molecular weight drugs or excipients forming a single-phase homogenous system in the amorphous form (Yarlagadda et al. 2021). The solubility improvement by CAM is a result of the high energy of the amorphous form at the time of dissolution (Karagianni et al. 2018). Co-formers used in the preparation stabilize the drug by molecular mixing, molecular interactions such as hydrogen bonding, salt formation, and π-π interactions (Liu et al. 2021). NRG (Fig. 1b), categorized as a GRAS, is a flavonoid derived from numerous citrus fruits (Yadav et al. 2020). The interaction of flavonoids such as naringenin, naringin, hesperidin, nobiletin, and hesperetin with the drugs that are enzyme or P-gp substrates results in inhibition or induction of efflux proteins and metabolic enzymes leading to higher plasma drug levels and better absorption (Hwang et al. 2015). NRG is known to improve the metabolism and absorption of several drugs (Shilpa et al. 2023). NRG as a co-former is reported to enhance the permeability of fexofenadine, talinolol, atorvastatin, and pyrazinamide by P-gp efflux inhibition through the formation of supersaturated solution of drugs in the gut (Teja et al. 2015; Nair et al. 2020; Prajapati et al. 2022; Uppala et al. 2022). The structural similarity of NRG with hydrophobic polyphenols may be an advantage for applying NRG to develop an amorphous formulation due to improved miscibility between them (Hatanaka et al. 2022). NRG delivers potential supramolecular H-bonding sites in the glycan portion recognized as crucial to induce disorder in the co-amorphous phase owing to its strong glass-forming ability. Such co-amorphous phases display a higher rate of dissolution and solubility by virtue of high energy confined within them (Teja et al. 2015).

In this study, a CAM of CUR and NRG in two molecular ratios of 1:1 and 1:2 was developed by quench cooling technique. The solid-state characterisation of the prepared CAM was carried out by DSC, PXRD, and FT-IR to determine the amorphous state and compatibility of the drugs. A stability-indicating reverse phase HPLC (RP-HPLC) method was developed to simultaneously estimate CUR and NRG, and the method was validated as per ICH Q2 (R1) guideline. A bioanalytical method was also developed in gradient mode to simultaneously estimate CUR and NRG in plasma. The content of drugs in CAM, solubility, in vitro drug release, and the in vivo pharmacokinetic studies were carried out using the developed method.

The individual methods were scrutinized and noted down as per the literature survey to be adapted for developing a new analytical method to simultaneously estimate CUR and NRG. The literature presented several methods for analysing CUR and NRG as individual entities. An immense exploration of the literature revealed few HPLC methods reported for the estimation of NRG in nanocapsules (Budel et al. 2020), nanosuspensions, and nanoparticles (Bhandari et al. 2019). Quite a limited HPLC methods have been reported for the simultaneous estimation of NRG with drugs such as atorvastatin and naringenin (Sowmya et al. 2019; Nair et al. 2020). Limited methods have been reported for the analysis of CUR simultaneously with piperine (Khismatrao et al. 2018), paclitaxel (Praveena and Guru 2021), quercetin (Patil and Mahajan 2022), mesalamine (Awasthi et al. 2022), cyclosporine (Desai et al. 2018), chlorin (Jain et al. 2023),

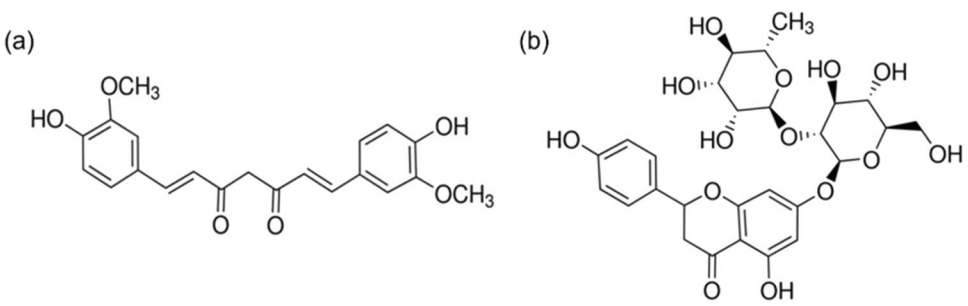

Fig. 1 **a** Structure of curcumin. Represents chemical structure of curcumin as per IUPAC nomenclature. **b** Structure of naringin. Represents chemical structure of naringin as per IUPAC nomenclature

and thymoquinone (Jagtap et al. 2021). Only two analytical methods are available for the estimation of CUR simultaneously with magnolol (Han et al. 2021), and piperine (Wang et al. 2019) in CAM. To date, there is no HPLC method available in existing literature for the concurrent determination of CUR and NRG.

Consequently, there is space for the development of an effective, sensitive, and stable HPLC method to simultaneously estimate CUR and NRG with better resolution of drugs in the mixture. To our acquaintance, this is the foremost stability-indicating RP-HPLC method for the estimation of CUR and NRG simultaneously in CAM as well as in plasma. Therefore, the present study aimed to develop and validate HPLC analytical method to simultaneously estimate CUR and NRG in the CAM. Further, the developed method is validated for parameters like accuracy, precision, robustness, and stability according to ICH Q2 (R1) guidelines. The optimized method is utilized for quantifying CUR and NRG, analysing solubility, and in vitro dissolution samples of the CUR in CAM. The method with few modifications was used to analyse plasma samples obtained from pharmacokinetic studies to determine the oral bioavailability of CUR in the presence of NRG.

Materials and Methods

Reagents

NRG hydrate and CUR were purchased from TCI chemicals, India. Glacial acetic acid and hydrochloric acid (37%) were purchased from Merck Ltd., India. HPLC grade methanol (minimum 99.9% purity) was purchased from Finar Ltd., India. Hydrogen peroxide 30% AR was procured from Loba Chemie Pvt. Ltd., India. Sodium hydroxide pellets (97% purity) were procured from Molychem, Mumbai, India. Unless stated, additional chemicals of analytical grade were used.

Chromatographic System and Conditions

The HPLC comprised of Shimadzu LC 2010CHT system equipped with autoinjector, column oven, and LC Solution 5.57 system control software. The separation of analytes was attained on a 4 µm Genesis C18 column with a 4.6 mm × 100 mm dimension. Mobile phase comprised of 48:52 and 75:25 v/v gradient ratio of 0.1% acetate buffer, adjusted to pH of 3.8 and methanol. MilliQ water was filtered through a 0.45-µm membrane filter before use. Flow rate was set to 0.5 ml/min for pumping of mobile phase through the column. The injection volume was 20 µl. The analytes were analysed at a single wavelength of 289 nm. MilliQ water to prepare buffer and sample was obtained from Millipore Elix® Advantage 3 purification system. The temperatures of column oven and autosampler were set at 25 and 4 °C, respectively.

Preparation of Standard and Sample Solutions

For the preparation of the stock solution, 10 mg each of CUR and NRG was dissolved in 10 ml methanol to attain 1000 µg/ml concentration. Subsequent dilutions of samples with a concentration between 0.125 and 16 µg/ml were prepared using the mobile phase.

Validation of Analytical Method

ICH Q2 (R1) guidelines were followed to validate the analytical method for specificity, system suitability, linearity, precision, accuracy, and robustness (ICH I. Q2 (R1) 2005).

Specificity

Three replicates of standard solution (CUR-NRG) in 10 µg/ml were injected to check the specificity.

System Suitability

Six replicates of standard solution (CUR-NRG) in 10 µg/ml were injected to check system suitability. The constraints, such as peak area, retention time, theoretical plate, and tailing factor, were analysed for acceptability.

Accuracy and Precision

Four replicates of standard solution (CUR-NRG) in 8, 10, and 12 µg/ml were injected to determine inter- and intra-day precision. The % RSD should be < 2% for the validity of the method. The % recovery of CUR and NRG at 8, 10, and 12 µg/ml concentrations indicates accuracy, which should be 98–102%.

Robustness

By presenting slight variations in the flow rate (± 0.1-unit), injection volume (20 to 19 µl and 21 µl), temperature (25 to 24 °C and 26 °C), and detector wavelength (289 to 288 and 290 nm), any variation in peak area, retention time, tailing factor, and theoretical plate count was observed. A standard solution (CUR-NRG) of 1 µg/ml was injected in triplicate to determine the robustness. In order for the method to be robust, % RSD should be < 2%.

Linearity

Suitable dilutions of 0.125, 0.5, 1, 2, 4, 8, and 16 µg/ml were prepared from the stock solution of CUR and NRG (100 µg/ml) using the mobile phase. The peak area of CUR and NRG against the respective concentration was plotted to obtain calibration curves.

Limit of Detection (LOD) and Limit of Quantification (LOQ)

LOD and LOQ calculations were done by means of the y-intercept standard deviation of regression lines and slope obtained from the calibration curve (54).

Bench-Top Stability

The stability was evaluated by injecting precision samples (1 µg/ml) in triplicates after 24 h together with fresh samples (1 µg/ml). The following equation was used to calculate the similarity index:

$$\text{Similarity index} = \frac{\text{peak area}_{\text{old std}} \times \text{amount}_{\text{new std}}}{\text{average peak area}_{\text{new std}} \times \text{amount}_{\text{old std}}}$$

where peak $\text{area}_{\text{old std}}$ and peak $\text{area}_{\text{new std}}$ are the peak areas of sample injected after 24 h and freshly prepared samples, respectively. $\text{Amount}_{\text{old std}}$ and $\text{amount}_{\text{new std}}$ correspond to the amount of precision sample and freshly prepared sample, respectively (Mutalik et al. 2021).

Stability Testing by Forced Degradation Studies

The sample of CUR-NRG (1 µg/ml) was subjected to acid-induced (0.1 and 1 N HCl), alkali-induced (0.1 and 1 N NaOH), thermal, and photolytic, in addition to oxidative (3% H_20_2) degradation.

Preparation of Acid-Induced and Alkaline-Induced Degradation Samples

The methanolic standard solution of CUR-NRG in 1000 µg/ml was treated with 3 ml of 0.1 N HCl and 1 N HCl distinctly. The acidic mixture was subjected to heating up to 24 h and 12 h, respectively, at 60 °C, following which they were neutralized by 0.1 and 1 N NaOH, respectively, and were diluted further and injected in triplicate.

For alkaline-induced hydrolysis, about 3 ml of 0.1 and 1 N NaOH were separately added to 1000 µg/ml standard solution of CUR-NRG. The alkaline mixture was heated for 24 h and 12 h, respectively, at 60 °C. They were neutralized by 0.1 and 1 N HCl, respectively, and were diluted further and injected in triplicate for analysis.

Preparation of Oxidation-Induced Degradation Product

The standard solution of CUR-NRG in 1000 µg/ml after treatment with 3% v/v H_2O_2 was placed in the dark for 24 h. The solution was injected in triplicate following suitable dilutions.

Preparation of Photolytic Degradation Product

The standard solution of CUR-NRG (1000 µg/ml) after 24 h of exposure to direct sunlight was analysed for photolytic degradation of drugs. The samples were suitably diluted and injected in triplicates to the column of HPLC.

Preparation of Thermal Degradation Product

The standard solution of CUR- NRG (1000 µg/ml) was exposed to 80 °C heat for a period of 24 h to study the thermal degradation of drugs. The samples were suitably diluted and injected in triplicates for analysis.

Chromatographic Conditions and Analytical Technique for the Simultaneous Estimation of CUR and NRG in Plasma

The same chromatographic conditions as that of the analytical method were followed for bioanalytical method development except for the gradient method: pH 3.5 0.1% acetate buffer and methanol in the ratio 45:55%v/v up to 5 min, 75:25%v/v from 7 to 13 min, and 45:55%v/v up to 17 min. The injection volume was set to 40 µl. The protein precipitation method was followed to extract the drug from plasma using chilled methanol. Resveratrol was selected as an internal standard. The samples were centrifuged at 10,000 rpm for 15 min at 4 °C, and the obtained supernatant was analysed by HPLC. The peak area of CUR and NRG along with internal standard against the respective concentration was plotted to obtain calibration curves.

Preparation of CAM

CAM of CUR and NRG was prepared by quench cooling. A total of 500 mg of CUR and NRG in 1:1 and 1:2 molar ratios were taken in a silica crucible and melted in a heating mantle at a temperature near the melting point of drugs and held for a minute, ascertaining the absolute melting of both the drugs. Further, the crucible was transferred into a pre-cooled glass desiccator and stored at − 80 °C for 3–4 h, following which the sample was scrapped gently and pulverized using a mortar and pestle to get a fine powder. The formulation was stored in a vacuum desiccator for further characterisation (Nair et al. 2020).

Characterisation of CAM

Differential Scanning Calorimetry (DSC)

The thermal characteristics were determined by DSC. In the analysis, pure drug samples, physical mixtures, and CAM were loaded separately in aluminium cups, placed inside DSC-60 (Shimadzu, Japan), and scanned at 30 to 300 °C. The nitrogen flow and heating rate were maintained at 40 ml/min and 10 °C/min, respectively, using Shimadzu TA- 60WS thermal analyser.

Powder X-ray Diffraction (PXRD)

The PXRD analysis of the pure drugs, physical mixtures, and CAM was performed using Rigaku X-ray diffractometer (Rigaku Co., Tokyo, Japan). A current of 15 mA and 40 kV voltage were maintained. The instrument was equipped with a monochromator made of graphite and a detector. About 10–20 mg of sample was analysed at 5–40° 2θ to obtain the diffractograms.

Fourier Transform-Infrared Spectroscopy (FT-IR)

The FT-IR spectra of CUR, NRG, physical mixtures, and CAM were obtained using Alpha II compact attenuated total reflectance FT-IR (ATR-FTIR) spectrometer (Bruker, USA). After the blank correlation, a small amount of the sample was placed on the ATR crystal, and the anvil was pressed down gently, ensuring sample contact with the crystal. The spectra were obtained upon scanning at a wave number ranging from 400 to 4000 cm^{-1} (Pisay et al. 2022).

Scanning Electron Microscopy (SEM) Analysis

SEM analysis using EVO MA18 coupled with Oxford EDS (Germany) was performed to visualize surface morphology of pure drugs and CAMs. The CUR, NRG, PM, and CAMs were placed individually on aluminium stub, and gold sputtering technique was followed (Kara et al. 2023).

Quantification of CUR and NRG in CAM

The drug content, solubility, and in vitro drug release of prepared CAM of CUR and NRG were estimated using the validated method. Five-milligram equivalent of CUR from CAM was dissolved in 10 ml methanol and diluted with mobile phase to obtain a 1 µg/ml concentration. Triplicates of CAM were injected to estimate CUR and NRG simultaneously, and the results were equated with standard CUR-NRG (1 µg/ml).

Solubility Analysis

The equilibrium solubility of CUR and the CAM was determined in the presence of USP phosphate buffer pH 6.8. An excessive amount of each sample was taken in an Eppendorf containing 1 ml of buffer in triplicates and placed for 24 h in a tube rotator at 50 rpm maintaining the room temperature. The samples were centrifuged at 10,000 rpm for 15 min, and the separated supernatant was analysed by HPLC.

In Vitro Drug Release Study

The release of pure CUR, CUR in physical mixtures, and CAM was performed in USP 50 mM phosphate buffer pH 6.8 and hydrochloric acid of pH 1.2. Drug release was monitored at 37 °C with 250–300 rpm in 20 ml buffer. One thousand microliters of samples at 5, 10, 15, 30, 60, 90, and 120 min were withdrawn, and the sink condition was maintained. Collected samples were centrifuged at 10,000 rpm for 15 min, and the supernatant obtained was analysed by HPLC (Navya et al. 2022).

Pharmacokinetic Studies

As per the CPESCA guidelines and upon approval by the Institutional Animal Ethics Committee (IAEC/KMC/45/2022), Manipal Academy of Higher Education (MAHE), the pharmacokinetic studies were carried out. The Sprague Dawley rats weighing 200–220 g were divided into CUR-, PM-, and CAM (1:2)-treated groups. Each group comprised three rats, and parallel study design was followed. The rats were subjected to fasting for 12 h prior to the studies with water accessibility. The CUR-treated group received 500 mg/kg of CUR in 0.5% w/v carboxyl methyl cellulose (CMC) solution. PM- and CAM-treated groups received 500 mg equivalent of CUR in 0.5% w/v CMC. The suspension (2 ml) was orally administered in rats by means of oral gavage. The blood samples were collected in heparinized tubes by retro-orbital bleeding method at a predetermined time interval of 1, 2, 4, 6, 8, 10, 12, and 24 h. The collected samples were centrifuged at 10,000 rpm, 4 °C for 10 min, to obtain the plasma and kept at − 80 °C till further study. GastroPlus™ software (version 9.7, Simulation Plus Inc. Lancaster, CA-USA) was applied to compute the pharmacokinetic parameters.

Results and Discussion

RP-HPLC Method Development

To begin with, acetonitrile and phosphate buffer, acetonitrile, and acetate buffer were tried in several ratios for the separation of individual drugs and the combination. The peak area of CUR was less in these trials, along with peak splitting. Further, methanol substituted acetonitrile was used with 0.1% acetate buffer in various ratios to analyse individual drugs and the combination. Acetate buffer (0.1%; pH adjusted to 3.8) showed symmetric peaks and better separation of the analytes. Combination of CUR and NRG, 10 µg each per 1 ml, was injected into the HPLC column after diluting it with mobile phase: methanol and acetate buffer (0.1% acetic acid; pH adjusted to 3.8) at various ratios. Gradient mode of elution with 0.5 ml/min flow rate showed better resolution of peaks. Both the peaks had a tailing factor of less than 2%. Chromatographic parameters along with a typical chromatogram of drugs are presented in Table 1 and Fig. 2, respectively.

Validation of the Analytical Method

ICH Q2 R1 guidelines were followed for validation of developed method.

System Suitability and Specificity

NRG and CUR eluted at 5.162 and 11.135 min, respectively, with high resolution and % RSD < 2%, as shown in Fig. 2.

Linearity

The calibration curve (area of CUR and NRG peaks versus the corresponding concentration) was plotted, and the linearity was observed in the concentration range of 0.125 to 16 µg/ml for both drugs. As shown in Table 2, the equations for linearity of CUR and NRG were observed to be $y = 24{,}715x + 10{,}443$ and $y = 61{,}289x + 2556.5$, respectively, with regression coefficient 1, indicative of the method to be valid and acceptable.

Accuracy and Precision

Known concentrations of combined solution of CUR and NRG at low (8 µg/ml), middle (10 µg/ml), and high (12 µg/ml) levels were injected to determine accuracy and precision. The % drug recovery ranged between 90 and 110%, and the % RSD was < 2.

LOD and LOQ

LOD and LOQ were observed to be 0.063 and 0.125 µg/ml, respectively.

Table 1 Chromatographic parameters along with gradient programme for the simultaneous estimation of CUR and NRG

Elution mode	Time (min)	Mobile phase	Ratio (%)
Gradient programme	0.01	Methanol	48
	0.01	Buffer	52
	2.50	Methanol	75
	2.50	Buffer	25
	8.00	Methanol	75
	8.00	Buffer	25
	13.00	Methanol	75
	13.00	Buffer	25
	15.00	Methanol	48
	15.00	Buffer	52
	17.00	Methanol	48
	17.00	Buffer	52
Parameter		Optimized result	
Column		Genesis C18 (100 × 4.6 mm × 4 µm)	
Mobile phase		Methanol: pH 3.8, 0.1% acetate buffer	
Flow rate		0.5 ml/min	
Temperature of column oven		25 °C	
Auto sampler temperature		4 °C	
Volume of injection		20 µl	
Detection wavelength		289 nm	
Run time		17 min	

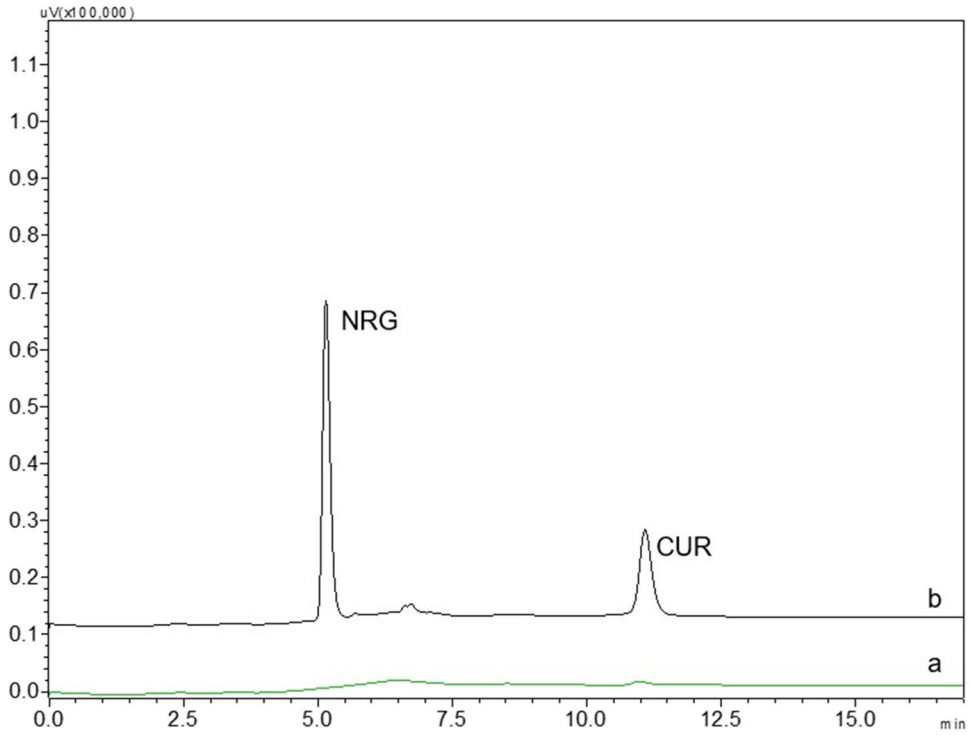

Fig. 2 Typical chromatogram representing (**a**) blank (**b**) NRG and CUR. Mobile phase was methanol-pH 3.8 0.1% acetate buffer with 0.5 ml/min a flow rate in gradient mode

Table 2 Summary of parameters of the HPLC method

Parameter	CUR	NRG
Linearity range (µg/ml)	0.125–16	0.125–16
Linearity equation	$y=24{,}715x+10{,}443$	$y=61{,}289x+2556.5$
R^2	0.9981	0.9996
Accuracy	97–100%	100–102%
Precision	0.4–0.64 (< 2.0%)	0.09–0.3 (< 2.0%)
LOD (µg/ml)	0.063	0.063
LOQ (µg/ml)	0.125	0.125

Robustness of the Method

Developed analytical method was deliberately assessed for robustness by varying chromatographic conditions. Varying the flow rate, temperature, injection volume, and wavelength resulted in slight variations in elution time, tailing factor, and theoretical plate count without significantly impacting peak area. The % RSD of < 2 designated the method robustness.

Stability Studies of CUR and NRG by Forced Degradation

CUR and NRG were subjected to forced degradation conditions to establish the potential of the method in autonomously resolving and measuring drug content to a wide range of stress-related conditions. Distinct chromatograms and a few degradation peaks at slightly shifted retention time were observed for both drugs. At 0.1 N HCl, CUR recovery was 41.94%, and NRG recovery was 63.29%. At 1 N HCl, CUR recovery was − 27.44%, and NRG recovery was 38.15%. At 0.1 N NaOH, CUR recovery was − 28.08%, and NRG recovery was 19.625%. At 1 N NaOH, CUR recovery was − 27.73%, and NRG recovery was 4.26%. At oxidative degradation, CUR recovery was 81.59%, and NRG recovery was 101.117%. Photolytic degradation of the CUR and NRG showed 87.42% and 91.89% recovery, respectively. The benchtop stability of the CUR and NRG showed 102.13% and 87.29% recovery, respectively. Thermal exposure of CUR and NRG to 80 °C showed 56.83 and 81.27% recovery, respectively.

Bioanalytical Method Development

Gradient mode of elution with 0.5 ml/min flow rate showed better resolution of peaks. All the peaks had a tailing factor of less than 2%. USFDA guidelines were followed for developing bioanalytical method by HPLC. The method displayed a retention time of 5.2 min and 15.14 min for NRG and CUR, respectively, while the internal standard resveratrol, showed a retention time of 7.7 min (Fig. 3). The method had linearity from 100 to 3200 ng/ml ($R^2=0.9586$ for NRG; $R^2=0.9869$ for CUR) with the lower limit of quantification (LLOQ) found to be 100 ng/ml. The chromatograms of QC samples are provided in Supplementary data.

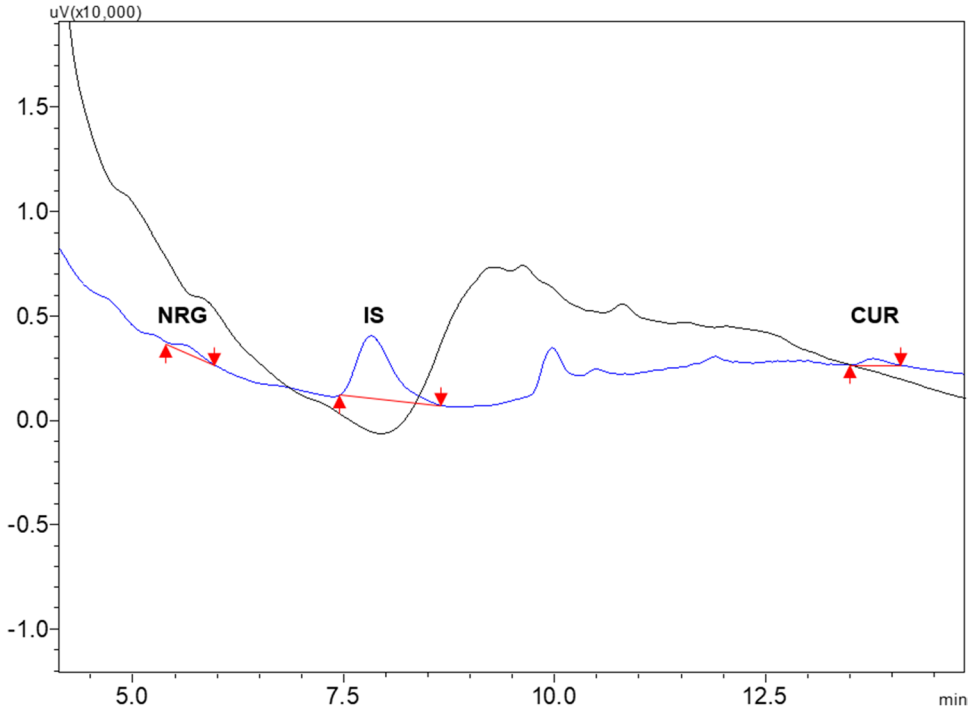

Fig. 3 Chromatogram representing NRG and CUR (100 ng/ml) eluting at 5.2 min and 15.10 min, respectively, internal standard (IS) resveratrol (400 ng/ml) at 7.7 min

Preparation and Characterisation of CAM

CAM of CUR and NRG (1:1 and 1:2 molar ratios) was prepared by quench cooling technique. The solid-state characterisation of CAM followed by drug content analysis and in vitro studies were carried out.

DSC

CUR, NRG, PM, and CAM were analysed by DSC to study their thermal characteristics. CUR presented a sharp endothermic peak at 182.44 °C, conforming to its crystallinity. NRG showed a broad peak corresponding to its semi-crystalline state; the crystalline PM exhibited endothermic peaks at 157–158 and 180 °C, corresponding to the melting points of NRG and CUR, respectively. The CAM (1:1 and 1:2) showed no endothermic peaks at 182.44 °C and 157–158 °C, respectively, confirming the conversion of CUR to an amorphous state during quench cooling as shown in Fig. 4.

PXRD

The X-ray diffractograms confirmed the formation of CAM. As per the PXRD data presented in Fig. 5, CUR showed characteristic peaks at 8.83°, 14.5°, 17.28°, 18.15°, 23.77°, 25.47°, and 28.89° representing its crystalline nature. NRG did not show any discrete peaks indicating its presence in the semi-crystalline state. The PM (1:1) showed characteristic peaks at 8.39°, 14.18°, 14.76°, 15.5°, 16.74°, 20.67°, 22.45°, 25.47°, and 28.83° whereas, PM (1:2) showed characteristic peaks at 8.59°, 14.16°, 14.74°, 15.39°, 16.75°, 17.78°, 19.06°, 21.38°, and 22.35° corresponding to crystalline CUR. The CAM of CUR and NRG displayed a halo spectrum confirming the amorphous phase of CAM, thus confirming the formation of CAM.

FT-IR

Any possible intermolecular interactions between the drugs in the CAM were identified by comparing CUR, NRG, and physical mixture spectra with the FT-IR spectra of CAM. The spectra of CUR, NRG, PM, and CAM of CUR and NRG are presented in Fig. 6. CUR showed characteristic peaks at 3496.56, 2358.22, 1625.35, 1596.89, 1423.40, and 1260.31 cm^{-1} corresponding to phenolic -OH stretching, O = C = O stretching, carbonyl stretching, C = C benzene ring, and C = C aromatic stretching. Distinctive peaks for NRG at 3344.84, 2922.10, 1640.41, 1511.07, and 1361.26 cm^{-1} indicated phenolic OH stretching, C-H aliphatic stretching, -C = O carbonyl stretching, aromatic bending, and -OH bending, respectively. The spectra of physical mixtures of CUR and NRG were referred to study the intermolecular interactions in the spectra of CAM. The O = C = O stretching in CUR observed at 2358.22 cm^{-1} shifted to 2362.75 cm^{-1} in CAM. A shift in the C = O carbonyl stretching was observed from 1625.35 to 1624.97 cm^{-1} in CAM. In the CAM (1:2), the O = C = O stretching was observed at 2362.75 cm^{-1}, and the C = O carbonyl stretching shifted from 1625.35 to 1628.45 cm^{-1}. The phenolic -OH stretching in CUR at 3496.56 cm^{-1} is

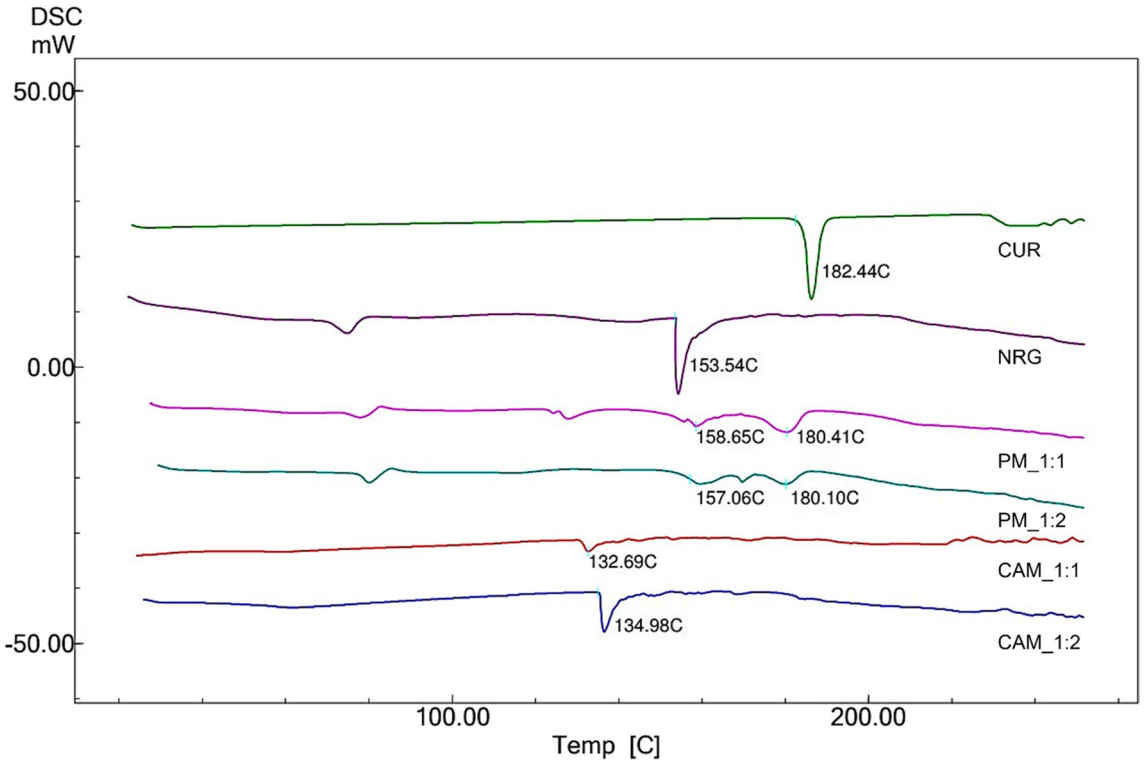

Fig. 4 DSC thermograms of crystalline CUR (186.29 °C), NRG, PM (NRG 157–158 °C and CUR 180 °C), and CAM of CUR and NRG

not observed in the spectra of CAM. The C-H stretching peak in NRG at 2922.10 cm^{-1} is not evident in CAM. It can be concluded that hydrogen bonding between phenolic -OH in CUR and the C-H aliphatic group in NRG is likely to be a driving force for the formation of CAM. Other characteristic peaks of the drugs were either shortened or broadened in CAM.

Scanning Electron Microscopy (SEM)

SEM analysis was done to visualize the surface morphology of pure drugs and CAMs. CUR exhibited a spherical structure (Fig. 7a), while NRG showed a sheet-like structure (Fig. 7b) as observed by J. Li et al. (Li et al. 2022). The PM showed characteristics of both CUR and NRG (Fig. 7c). The CAMs showed irregularly shaped blocks representing the presence of drugs in their amorphous form (Fig. 7d and e). The structural irregularity in CAMs compared to CUR and PM may be associated with the thermodynamic due to quench cooling (Li et al. 2021). The irregular structures could increase surface area thereby enhancing solubility of CUR (Mohapatra et al. 2021).

Quantification of CUR and NRG in CAM

The developed method was able to estimate CUR and NRG simultaneously. The CAM prepared by the quench cooling technique was evaluated for drug content. The CAM showed 64.42 and 92.24% of CUR and NRG, respectively.

Solubility Studies

Solubility studies of CUR, physical mixtures, and CAM were carried out in USP pH 6.8 phosphate buffer. The samples were analysed by HPLC. The solubility of CUR and NRG was found to be 1.35 and 13.8 µg/ml, respectively, and that of CUR in physical mixtures (1:1 and 1:2) was 22 and 41 µg/ml, respectively. The solubility of CUR in CAM (1:1 and 1:2) was 81.5 and 252.5 µg/ml, respectively, indicating significant improvement in the solubility of CUR compared to its crystalline counterpart.

In Vitro Drug Release Studies

The release studies were performed at sink conditions to determine the behaviour of crystalline CUR and CUR in CAM in an aqueous medium. The release profile of

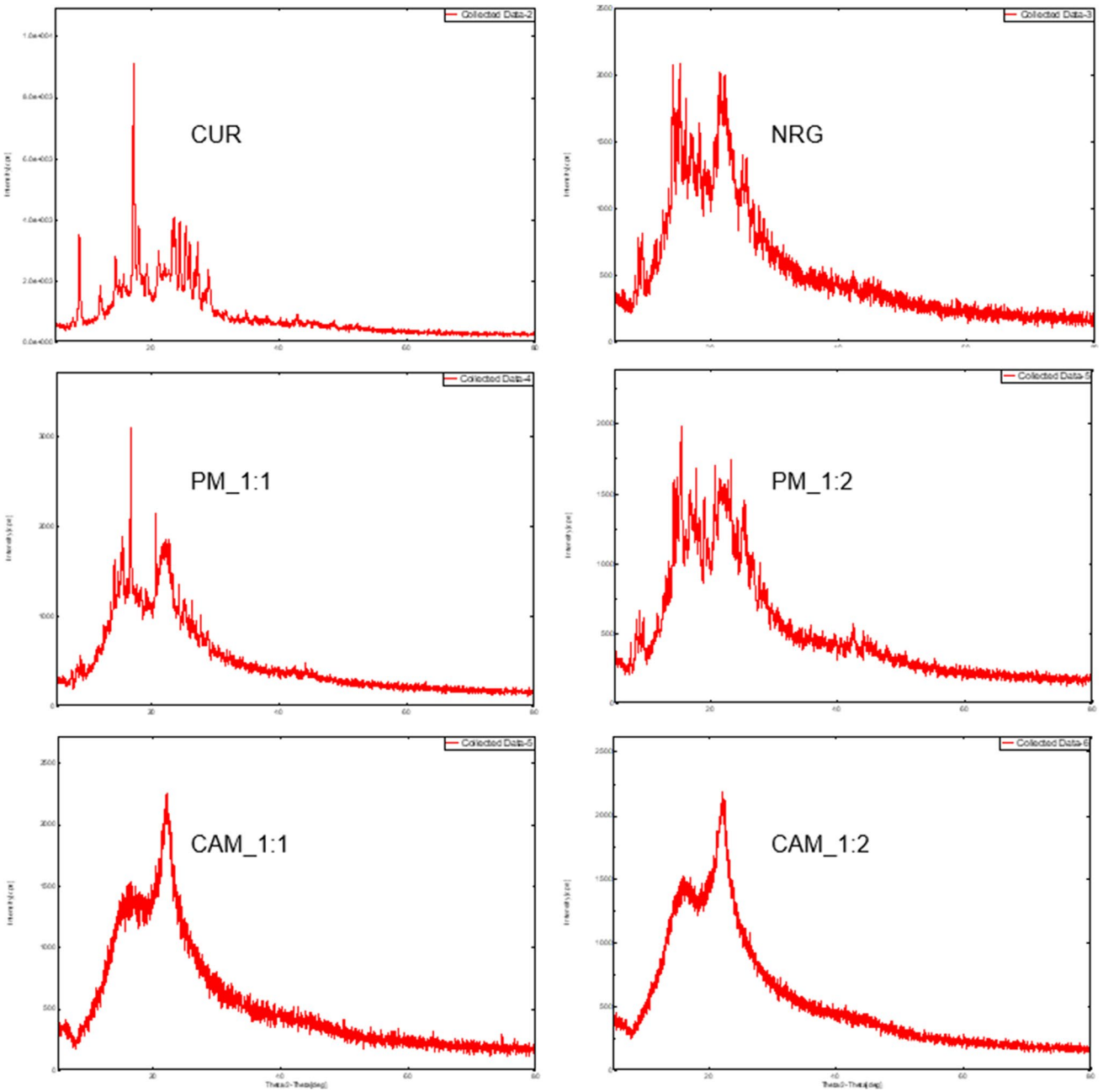

Fig. 5 XRD diffractograms of crystalline CUR, NRG, physical mixtures, and CAM of CUR and NRG (1:1 and 1:2)

CAM was compared with the physical mixtures of CUR and NRG. It was deceptive that the release of CUR in both acidic and basic buffers (Fig. 8a and b, respectively) increased with time, attaining a steady state after 2 h. The CAM (1:2) displayed a maximum rate of dissolution of CUR compared to CAM (1:1). The physical mixtures exhibited a significantly lesser extent of release of CUR.

Pharmacokinetic Studies

It is necessary to render the advantage of solubility into oral bioavailability to measure the effectiveness of CAM. CUR is a P-gp substrate and undergoes phase II metabolism, CAM improves the oral bioavailability of CUR due to its presence in an amorphous state. The two possible

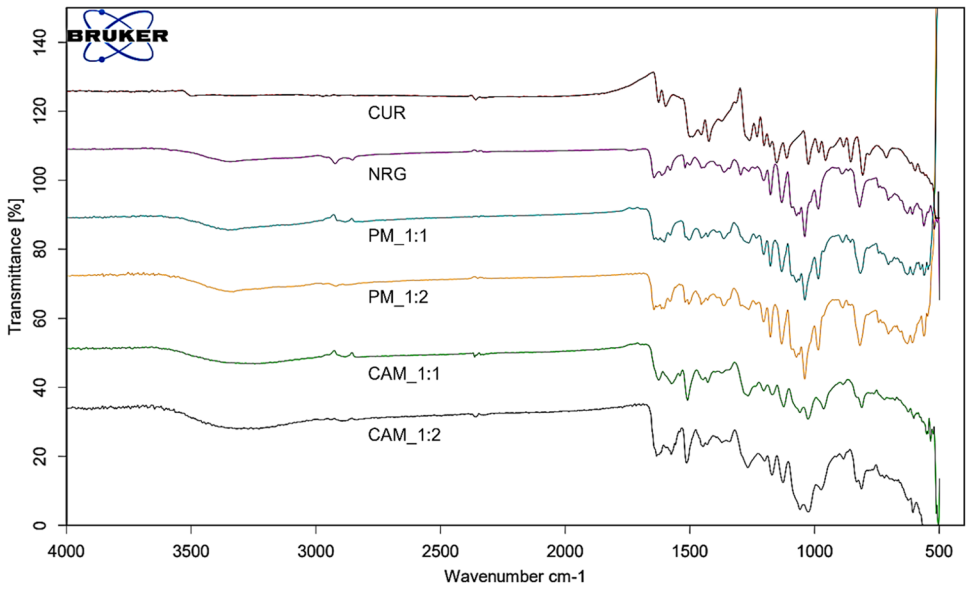

Fig. 6 FTIR spectra of crystalline CUR, NRG, physical mixtures, and co-amorphous formulations of CUR and NRG

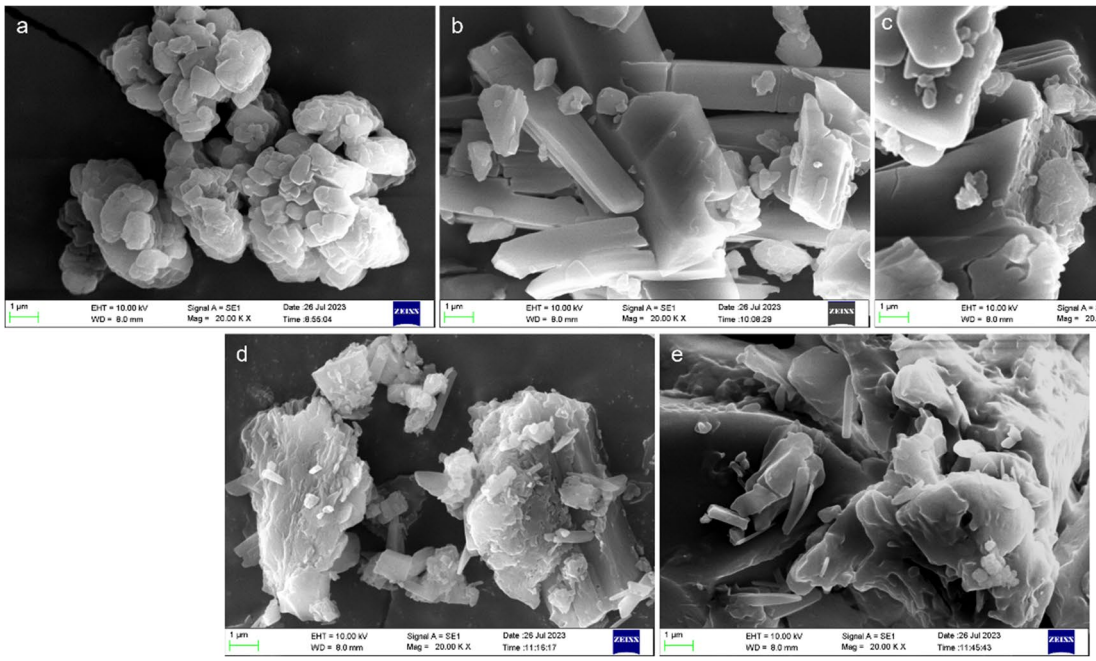

Fig. 7 SEM images of **a** CUR, **b** NRG, **c** PM, **d** CAM 1:1, and **e** CAM 1:2

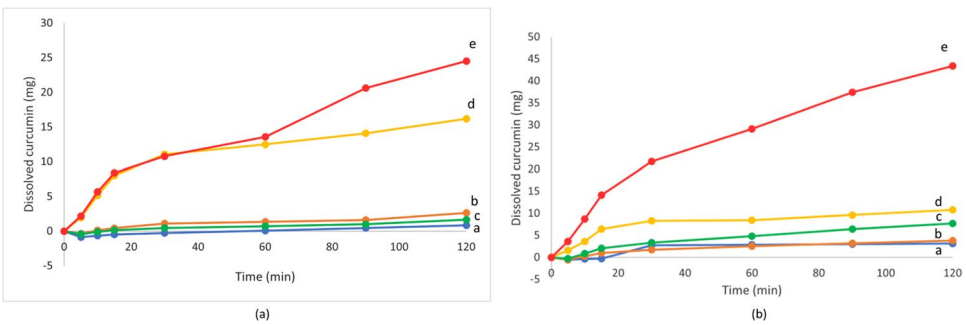

Fig. 8 **a** Drug release profiles of (a) crystalline CUR, CUR in physical mixtures (b) 1:1 and (c) 1:2, and CUR in CAM (d) 1:1 and (e) 1:2 in pH 1.2 HCl. **b** Drug release profiles of (a) crystalline CUR, CUR in physical mixtures (b) 1:1 and (c) 1:2, and CUR in CAM (d) 1:1 and (e) 1:2 in USP pH 6.8 phosphate buffer

reasons for improving oral bioavailability of CUR could be the improved solubility and P-gp efflux inhibition in the presence of NRG, abetting rapid transit into the blood (Yarlagadda et al. 2023). During pharmacokinetic study, CUR demonstrated a maximum plasma concentration of 45.37 µg/ml at 6 h. Based on in vitro studies, CAM 1:2 showed better efficacy compared to CAM 1:1 and was chosen for in vivo pharmacokinetic study. CUR in PM and CUR in CAM exhibited a maximum concentration in plasma of 59.76 µg/ml at 8 h and 113.76 µg/ml at 6 h, respectively (Fig. 9). The pharmacokinetic parameters were determined using GastroPlus™ software, employing non-compartmental and one-compartmental model. Table 3 shows the pharmacokinetic parameters of CUR, PM, and CAM (1:2). As per the non-compartmental and one-compartment analysis, CAM showed 14.9- and 7.8-fold increase in the AUC than the pure CUR and PM, respectively. The C_{max} of CUR in CAM was increased by 2.75 and 1.46-fold compared to pure CUR and PM, respectively. The enhanced plasma concentration exhibited by CAM of CUR and NRG demonstrates CUR's improved solubility and oral bioavailability.

Conclusion

CUR has been widely used in food industries, cosmetic preparations, and pharmaceutical arena. NRG and CUR are used in the development of functional food that aids in the treatment and management of various ailments. In this work, sensitive, robust, stability-indicating analytical method is developed and validated for the quantification of CUR and NRG simultaneously. Both the drugs eluted within 17 min minimising the analysis time and solvent usage resulting in a cost-effective method. Lower limits of detection and quantification with a wide linearity range represent method sensitivity. Forced degradation analysis in the presence of various stress factors such as acid, alkali, heat, oxidation, and light concluded that both the drugs are stable. CAM of CUR and NRG was prepared by quench cooling. DSC and XRPD confirmed the conversion of CUR to an amorphous form. FT-IR revealed hydrogen bonding between CUR and NRG. The developed method was applied in quantifying CUR and NRG, solubility studies, and in vitro drug release studies. The solubility and drug release of CUR in CAM were

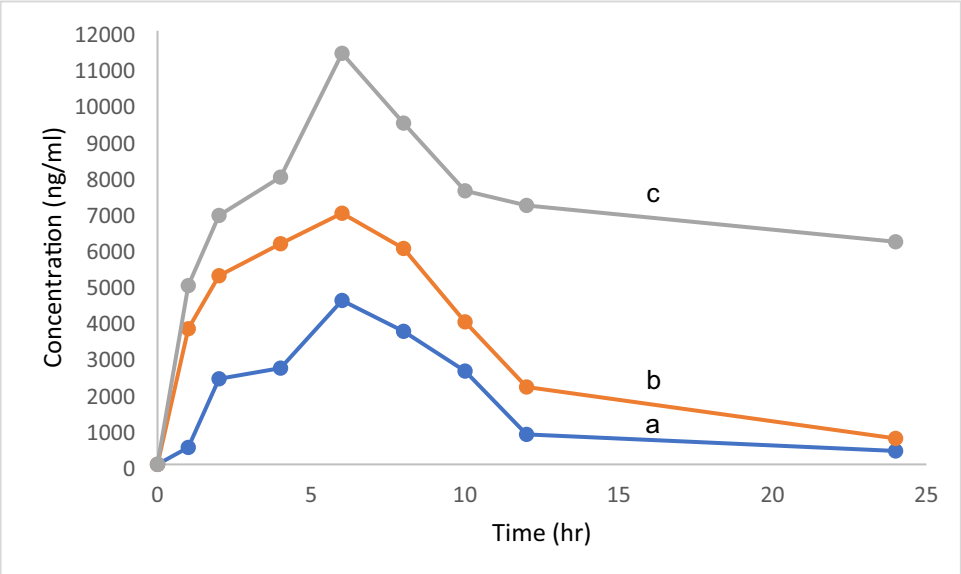

Fig. 9 Plasma concentration and time profile (a) CUR, (b) CUR in PM, and (c) CUR in CAM 1:2

Table 3 Pharmacokinetic parameters after administering a single dose of CUR equivalent to 500 mg/kg orally ($n=3$)

Samples	Non-compartment model parameters			One-compartment simulation linear model parameters			
	$AUC_{0-\infty}$ (µg/h/ml)	MRT (h)	$t_{1/2}$ (h)	$AUC_{0-\infty}$ (µg/h/ml)	MRT (h)	C_{max} (µg/ml/mg)	$t_{1/2}$ (h)
CUR	44.56	11.98	10.36	44.56	5.070	0.0069	3.514
PM	84.75*	10.45	7.617	84.75	7.618	0.013	5.280
CAM	663.9*	79.13*	55*	663.9*	36.59*	0.019*	25.36*

*Represents a significant difference in comparison to CUR and PM

*$p<0.05$ significantly different

significantly enhanced compared to crystalline CUR. The increase in the release of CUR from CAM (1:2) could be due to improved solubility and rate of dissolution of amorphous forms than crystalline counterpart. NRG is a glass-forming agent due to the presence of abundant hydroxyl groups in the glycan part that offers possible supramolecular hydrogen bonding sites, vital for inducing disorder in the co-amorphous phases. The profound effect of co-former NRG on the amorphous state of CUR, its solubility, and oral bioavailability is thereby evident from the study. However, further characterisation and evaluation studies are required to evaluate the efficacy of the formulations.

Supplementary Information The online version contains supplementary material available at https://doi.org/10.1007/s12161-024-02606-9.

Acknowledgements The authors are thankful for Manipal College of Pharmaceutical Sciences, Manipal Academy of Higher Education, Manipal, for providing the necessary facilities to carry out the research. The authors also acknowledge Ashutosh Gupta, Research Scholar, and Dr. Sudheer Moorkoth, Head and Professor, Department of Pharmaceutical Quality Assurance, MCOPS, Manipal, for the help.

Author Contribution Pooja Mallya: methodology, validation, conceptualization, analysis, and writing—original draft. Dani Lakshman Yarlagadda: methodology, investigation, conceptualization, and writing—review and editing. Shaila Lewis: investigation, supervision, critical revision of final draft, and approved the version to be published. All authors reviewed the manuscript.

Funding Open access funding provided by Manipal Academy of Higher Education, Manipal

Data Availability Data will be made available if requested.

Declarations

Ethics Approval and Consent to Participate The animal study was approved by the Institutional Animal Ethics Committee (IAEC/KMC/45/2022), Manipal Academy of Higher Education (MAHE).

Competing Interests The authors declare no competing interests.

References

Alam S, Sarker MMR, Sultana TN, Chowdhury MNR, Rashid MA, Chaity NI, Zhao C, Xiao J, Hafez EE, Khan SA, Mohamed IN (2022) Antidiabetic phytochemicals from medicinal plants: prospective candidates for new drug discovery and development. Front Endocrinol 13. https://doi.org/10.3389/fendo.2022.800714

Ali T, Shah Z, Bashir R, Bader GN (2019) The traditional medicine and phytoconstituents from natural products for liver disease: a review. J Drug Deliv Ther 9(2):484–488. https://doi.org/10.22270/jddt.v9i2.2387

Asati V (2022) Perspectives of anti-cancer phytoconstituents in pharmacotherapy. Int J Med Pharm Sci 12(3). https://doi.org/10.31782/ijmps.2022.12301

Awasthi A, Kumar A, Kumar R, Vishwas S, Khursheed R, Kaur J, Corrie L, Kumar B, Gulati M, Kumar D, Kaushik M, Gupta G, Prasher P, Chellappan DK, Kumar AP, Dua K, Singh SK (2022) RP-HPLC method development and validation for simultaneous estimation of mesalamine and curcumin in bulk form as well as nanostructured lipid carriers. S Afr J Bot 151:529–537. https://doi.org/10.1016/j.sajb.2022.05.044

Balan A, Moga MA, Dima L, Dinu CG, Martinescu CC, Panait DE, Irimie CA, Anastasiu CV (2021) An overview on the conservative management of endometriosis from a naturopathic perspective: phytochemicals and medicinal plants. Plants 10(3):1–31. https://doi.org/10.3390/plants10030587

Behl T, Gupta A, Albratty M, Najmi A, Meraya AM, Alhazmi HA, Anwer MK, Bhatia S, Bungau SG (2022) Alkaloidal phytoconstituents for diabetes management: exploring the unrevealed potential. Molecules 27(18). https://doi.org/10.3390/molecules27185851

Bhandari R, Kuhad A, Paliwal JK, Kuhad A (2019) Development of a new, sensitive, and robust analytical and bio-analytical RP-HPLC method for in-vitro and in-vivo quantification of naringenin in polymeric nanocarriers. J Anal Sci Technol 10(1). https://doi.org/10.1186/s40543-019-0169-1

Bolat ZB, Islek Z, Demir BN, Yilmaz EN, Sahin F, Ucisik MH (2020) Curcumin- and piperine-loaded emulsomes as combinational treatment approach enhance the anticancer activity of curcumin on HCT116 colorectal cancer model. Front Bioeng Biotechnol 8. https://doi.org/10.3389/fbioe.2020.00050

Budel RG, da Silva DA, Moreira MP, Dalcin AJF, da Silva AF, Nazario LR, Majolo JH, Lopes LQS, Santos RCV, Antunes Soares FA, da Silva RS, Gomes P, Boeck CR (2020) Toxicological evaluation of naringin-loaded nanocapsules in vitro and in vivo. Colloids Surf B: Biointerfaces 188. https://doi.org/10.1016/j.colsurfb.2019.110754

Bulboacă AE, Porfire AS, Tefas LR, Boarescu PM, Bolboacă SD, Stănescu IC, Bulboacă AC, Dogaru G (2019) Liposomal curcumin is better than curcumin to alleviate complications in experimental diabetic mellitus. Molecules 24(5). https://doi.org/10.3390/molecules24050846

Chen F, & Liu Q (2022) Demystifying phytoconstituent-derived nanomedicines in their immunoregulatory and therapeutic roles in inflammatory diseases. Adv Drug Deliv Rev 186. https://doi.org/10.1016/j.addr.2022.114317

Chorosho SH, Malik N, Panesar G, Kumari P, Jangra S, Kaur R, Al-Ghamdi MS, Albishi TS, Chopra H, Singh R, Murthy HCA (2023) Phytochemicals: alternative for infertility treatment and associated conditions. Oxid Med Cell Longev 2023:1327562. https://doi.org/10.1155/2023/1327562

Das A, Pandita D, Jain GK, Agarwal P, Grewal AS, Khar RK, Lather V (2021) Role of phytoconstituents in the management of COVID-19. Chem-Biol Interact 341. https://doi.org/10.1016/j.cbi.2021.109449

Desai N, Momin M, Singh U, Khan T, & Sherje A (2018) Analytical method development and validation for simultaneous estimation of curcumin and cyclosporine by RP-HPLC. Int J Pharm Pharm Sci 26–33. https://doi.org/10.22159/ijpps.2019v11i2.28975

ICH I. Q2 (R1) (2005) Validation of analytical procedures: text and methodology. International conference on harmonization. Geneva, pp 1–13

Ghelani H, Razmovski-Naumovski V, Chang D, Nammi S (2019) Chronic treatment of curcumin improves hepatic lipid metabolism and alleviates the renal damage in adenine-induced chronic kidney disease in Sprague-Dawley rats. BMC Nephrol 20(1). https://doi.org/10.1186/s12882-019-1621-6

Han J, Wei Y, Li L, Song Y, Pang Z, Qian S, Zhang J, Gao Y, Heng W (2023) Gelation elimination and crystallization inhibition by co-amorphous strategy for amorphous curcumin. J Pharm Sci 112(1):182–94. https://doi.org/10.1016/j.xphs.2022.07.014

Han J, Li L, Su M, Heng, W, Wei Y, Gao Y, Qian S (2021) Deaggregation and crystallization inhibition by small amount of polymer addition for a co-amorphous curcumin-magnolol system. Pharmaceutics 13(10). https://doi.org/10.3390/pharmaceutics13101725

Hatanaka Y, Uchiyama H, Kadota K, Tozuka Y (2022) Designing amorphous formulations of polyphenols with naringin by spray-drying for enhanced solubility and permeability. Adv Powder Technol 33(11):103627. https://doi.org/10.1016/j.apt.2022.103627

Hwang, SL, Shih PH, Yen GC (2015). Citrus flavonoids and effects in dementia and age-related cognitive decline. In Diet Nutr Dementia Cognitive Decline 869–878. https://doi.org/10.1016/B978-0-12-407824-6.00080-X

Ipar VS, Dsouza A, Devarajan PV (2019) Enhancing curcumin oral bioavailability through nanoformulations. Eur J Drug Metab Pharmacokinet 44(4):459–480. https://doi.org/10.1007/s13318-019-00545-z

Jagtap P, Mahajan N, Parte A, Pananchery J, Jain A (2021) RP-HPLC method development and validation for simultaneous estimation of thymoquinone and curcumin in dosage form. J Pharm Res Int 53–62. https://doi.org/10.9734/jpri/2021/v33i59b34352

Jain R, Dubey SK, & Singhvi G (2023) Stability indicating validated high-performance liquid chromatography method for simultaneous estimation of chlorin e6 and curcumin in bulk and drug-loaded lipidic nanoformulation. Sep Sci Plus 6(1). https://doi.org/10.1002/sscp.202200107

Jiang T, Ghosh R, Charcosset C (2021) Extraction, purification and applications of curcumin from plant materials-a comprehensive review. Trends Food Sci Technol 112:419–430. https://doi.org/10.1016/j.tifs.2021.04.015

Joshi M, Prabhakar B (2020) Phytoconstituents and pharmaco-therapeutic benefits of pitaya: a wonder fruit. J Food Biochem 44(7). https://doi.org/10.1111/jfbc.13260

Kancherla N, Dhakshinamoothi A, Chitra K, Komaram RB (2019) Preliminary analysis of phytoconstituents and evaluation of anthelminthic property of Cayratia auriculata (in vitro). Maedica 14(4):350–356. https://doi.org/10.26574/maedica.2019.14.4.350

Kara DD, Bangera PD, Mehta CH, Tanvi K, Rathnanand M (2023) In silico screening as a tool to prepare drug-drug cocrystals of ibrutinib-ketoconazole: a strategy to enhance their solubility profiles and oral bioavailability. AAPS PharmSciTech 24(6):164. https://doi.org/10.1208/s12249-023-02621-9

Karagianni A, Kachrimanis K, Nikolakakis I (2018) Co-amorphous solid dispersions for solubility and absorption improvement of drugs: composition, preparation, characterization and formulations for oral delivery. Pharmaceutics 10(3) https://doi.org/10.3390/pharmaceutics10030098

Kaur B, Rolta R, Salaria D, Kumar B, Fadare OA, da Costa RA, Ahmad A, Al-Rawi MBA, Raish M, Rather IA (2022) An in silico investigation to explore anti-cancer potential of Foeniculum vulgare Mill. Phytoconstituents for the Management of Human Breast Cancer. Molecules 27(13). https://doi.org/10.3390/molecules27134077

Khan A, Qadir A, Ali F, Aqil M (2021) Phytoconstituents based nanomedicines for the management of psoriasis. J Drug Deliv Sci Technol 64. https://doi.org/10.1016/j.jddst.2021.102663

Khismatrao A, Bhairy S, Hirlekar R (2018) Development and validation of RP-HPLC method for simultaneous estimation of curcumin and piperine. Int J Appl Pharm 10(5):43–48. https://doi.org/10.22159/ijap.2018v10i5.21140

Li YW, Zhang HM, Cui BJ, Hao CY, Zhu HY, Guan J, Wang D, Jin Y, Feng B, Cai JH, Qi XR (2021) "Felodipine-indomethacin" co-amorphous supersaturating drug delivery systems:"Spring-parachute" process, stability, in vivo bioavailability, and underlying molecular mechanisms. Eur J Pharm Biopharm 166:111–25. https://doi.org/10.1016/j.ejpb.2021.05.030

Li J, Li M, Jiang H, Chen L, Zhang N, Zhou YQ, Guo QX (2022) Selection of bionic co-former improves the dissolution of neohesperidin via co-amorphous solid dispersion with naringin. Eur J Pharm Biopharm 181:159–72. https://doi.org/10.1016/j.ejpb.2022.11.013

Lin L, Li C, Zhang D, Yuan M, Chen CH, Li M (2020) Synergic effects of berberine and curcumin on improving cognitive function in an alzheimer's disease mouse model. Neurochem Res 45(5):1130–1141. https://doi.org/10.1007/s11064-020-02992-6

Liu Z, Smart JD, Pannala AS (2020) Recent developments in formulation design for improving oral bioavailability of curcumin: a review. J Drug Deliv Sci Technol 60:102082. https://doi.org/10.1016/j.jddst.2020.102082

Liu J, Grohganz H, Löbmann K, Rades T, Hempel NJ (2021) Co-amorphous drug formulations in numbers: recent advances in co-amorphous drug formulations with focus on co-formability, molar ratio, preparation methods, physical stability, in vitro and in vivo performance, and new formulation strategies. Pharmaceutics 13(3). https://doi.org/10.3390/pharmaceutics13030389

Luo ED, Jiang HM, Chen W, Wang Y, Tang M, Guo WM, Diao HY, Cai NY, Yang X, Bian Y, Xing SS (2023) Advancements in lead therapeutic phytochemicals polycystic ovary syndrome: a review. Front Pharmacol 13. https://doi.org/10.3389/fphar.2022.1065243

Mardani R, Hamblin MR, Taghizadeh M, Banafshe HR, Nejati M, Mokhtari M, Borran S, Davoodvandi A, Khan H, Jaafari MR, Mirzaei H (2020) Nanomicellar-curcumin exerts its therapeutic effects via affecting angiogenesis, apoptosis, and T cells in a mouse model of melanoma lung metastasis. Pathol Res Pract 216(9). https://doi.org/10.1016/j.prp.2020.153082

Mizoguchi R, Waraya H, Hirakura Y (2019) Application of co-amorphous technology for improving the physicochemical properties of amorphous formulations. Mol Pharm 16(5):2142–2152. https://doi.org/10.1021/acs.molpharmaceut.9b00105

Mohapatra TK, Moharana AK, Swain RP, Subudhi BB (2021) Coamorphisation of acetyl salicylic acid and curcumin for enhancing dissolution, anti-inflammatory effect and minimizing gastro toxicity. J Drug Deliv Sci Technol 61:102119. https://doi.org/10.1016/j.jddst.2020.102119

Mutalik SP, Mullick P, Pandey A, Kulkarni SS, Mutalik S (2021) Box-Behnken design aided optimization and validation of developed reverse phase HPLC analytical method for simultaneous quantification of dolutegravir sodium and lamivudine co-loaded in nanoliposomes. J Sep Sci 44(15):2917–2931. https://doi.org/10.1002/jssc.202100152

Nair A, Varma R, Gourishetti K, Bhat K, Dengale S (2020) Influence of preparation methods on physicochemical and pharmacokinetic properties of co-amorphous formulations: the case of co-amorphous atorvastatin: naringin. J Pharm Innov 15(3):365–379. https://doi.org/10.1007/s12247-019-09381-9

Nakonieczna S, Grabarska A, Kukula-koch W (2020) The potential anticancer activity of phytoconstituents against gastric cancer—a review on in vitro, in vivo, and clinical studies. Int J Mol Sci 21(21):1–27. https://doi.org/10.3390/ijms21218307

Navya NS, Dengale SJ, Mutalik S, Bhat K (2022) Raloxifene HCl–quercetin co-amorphous system: preparation, characterization, and investigation of its behaviour in phosphate buffer. Drug Dev Ind Pharm 48(6):227–238. https://doi.org/10.1080/03639045.2022.2104308

Norooznezhad F, Rodriguez-Merchan EC, Asadi S, Norooznezhad AH (2020) Curcumin: hopeful treatment of hemophilic arthropathy via inhibition of inflammation and angiogenesis. Expert Rev Hematol 13(1):5–11. https://doi.org/10.1080/17474086.2020.1685867

Patil N, Mahajan H (2022) Development and validation of RP-HPLC method for simultaneous qualitative and quantitative estimation of curcumin and quercetin in bulk mixture. Indian J Pharm Educ Res 56(1):247–254. https://doi.org/10.5530/ijper.56.1.29

Pisay M, Bhaskar KV, Mehta CH, Nayak UY, Koteshwara KB, Mutalik S (2022) Drug-carrier miscibility in solid dispersions of glibenclamide and a novel approach to enhance its solubility using an effervescent agent. AAPS PharmSciTech 23(8). https://doi.org/10.1208/s12249-022-02437-z

Prajapati B, Maji I, Kumar R, Tomar D, Khatri DK, Madan J, Singh PK (2022) Strategy to counteract the pyrazinamide induced hepatotoxicity by developing naringin based co-amorphous system with supplementary benefits. J Drug Deliv Sci Technol 69:103181. https://doi.org/10.1016/j.jddst.2022.103181

Praveena J, Guru BR (2021) Simultaneous estimation of paclitaxel and curcumin in nano-formulation: stability analysis of drugs, optimization and validation of HPLC method. J Appl Pharm Sci 11(3):071–083. https://doi.org/10.7324/JAPS.2021.110308

Sayed N, Khurana A, Godugu C (2019) Pharmaceutical perspective on the translational hurdles of phytoconstituents and strategies to overcome. J Drug Deliv Sci Technol 53:101201. https://doi.org/10.1016/j.jddst.2019.101201

Shilpa VS, Shams R, Dash KK, Pandey VK, Dar AH, Ayaz Mukarram S, Harsányi E, Kovács B (2023) Phytochemical properties, extraction, and pharmacological benefits of naringin: a review. Molecules 28(15):5623. https://doi.org/10.3390/molecules28155623

Singh AK, Rai SN, Maurya A, Mishra G, Awasthi R, Shakya A, Chellappan DK, Dua K, Vamanu E, Chaudhary SK, Singh MP (2021) Therapeutic potential of phytoconstituents in management of Alzheimer's disease. Evid-Based Complementary Altern Med 2021. https://doi.org/10.1155/2021/5578574

Sohaei S, Amani R, Tarrahi MJ, Ghasemi-Tehrani H (2019) The effects of curcumin supplementation on glycemic status, lipid profile and hs-CRP levels in overweight/obese women with polycystic ovary syndrome: a randomized, double-blind, placebo-controlled clinical trial. Complementary Ther Med 47. https://doi.org/10.1016/j.ctim.2019.102201

Sowmya N, Haraprasad N, Hema BP (2019) Exploring the total flavonoid content of peels of Citrus auriantum, Citrus maxima and Citrus sinensis using different solvents and HPLC-analysis of flavonones—Naringin and Naringenin in peels of Citrus maxima. Pharma Innov 8:12–7

Suresh K, Chaitanya Mannava MKC, Nangia A (2014) A novel curcumin-artemisinin coamorphous solid: physical properties and pharmacokinetic profile. RSC Adv 4(102):58357–58361. https://doi.org/10.1039/c4ra11935e

Tabanelli R, Brogi S, Calderone V (2021) Improving curcumin bioavailability: current strategies and future perspectives. Pharmaceutics 13(10). https://doi.org/10.3390/pharmaceutics13101715

Tagde P, Islam F, Tagde S, Shah M, Hussain ZD, Rahman MH, Najda A, Alanazi IS, Germoush MO, Mohamed HRH, Algandaby MM, Nasrullah MZ, Kot N, Abdel-Daim MM (2021) The multifaceted role of curcumin in advanced nanocurcumin form in the treatment and management of chronic disorders. Molecules 26(23). https://doi.org/10.3390/molecules26237109

Teja A, Musmade PB, Khade AB, Dengale SJ (2015) Simultaneous improvement of solubility and permeability by fabricating binary glassy materials of talinolol with naringin: solid state characterization, in-vivo in-situ evaluation. Eur J Pharm Sci 78:234–244. https://doi.org/10.1016/j.ejps.2015.08.002

Temkar V, Menon S (2022) Combination of phytochemicals in the management of polycystic ovarian syndrome induced in rats. Phcog Commn 12(4):148–153. https://doi.org/10.5530/pc.2022.4.29

Uppala S, Vullendula SKA, Yarlagadda DL, Dengale SJ (2022) Exploring the utility of co-amorphous materials to concurrently improve the solubility and permeability of Fexofenadine. J Drug Deliv Sci Technol 72. https://doi.org/10.1016/j.jddst.2022.103431

Wang R, Han J, Jiang A, Huang R, Fu T, Wang L, Zheng Q, Li W, Li J (2019) Involvement of metabolism-permeability in enhancing the oral bioavailability of curcumin in excipient-free solid dispersions co-formed with piperine. Int J Pharm 561:9–18. https://doi.org/10.1016/j.ijpharm.2019.02.027

Wdowiak K, Pietrzak R, Tykarska E, Cielecka-Piontek J (2023) Hot-melt extrusion as an effective technique for obtaining an amorphous system of curcumin and piperine with improved properties essential for their better biological activities. Molecules 28(9). https://doi.org/10.3390/molecules28093848

Xu H, Wu T, Huang L (2021) Therapeutic and delivery strategies of phytoconstituents for renal fibrosis. Adv Drug Deliv Rev 177. https://doi.org/10.1016/j.addr.2021.113911

Xue F, Li X, Qin L, Liu X, Li C, Adhikari B (2021) Anti-aging properties of phytoconstituents and phyto-nanoemulsions and their application in managing aging-related diseases. Adv Drug Deliv Rev 176. https://doi.org/10.1016/j.addr.2021.113886

Yadav M, Sehrawat N, Singh M, Upadhyay SK, Aggarwal D, Sharma AK (2020) Cardioprotective and hepatoprotective potential of citrus flavonoid naringin: current status and future perspectives for health benefits. Asian J Biol Life Sci 9(1):1–5. https://doi.org/10.5530/ajbls.2020.9.1

Yarlagadda DL, Anand VS, Nair AR, Dengale SJ, Pandiyan S, Mehta CH, Manandhar S, Nayak UY, Bhat K (2023) A computational-based approach to fabricate Ceritinib co-amorphous system using a novel co-former rutin for bioavailability enhancement. Eur J Pharm Biopharm 190:220–30

Yarlagadda DL, Sai Krishna Anand V, Nair AR, Navya Sree KS, Dengale SJ, Bhat K (2021) Considerations for the selection of co-formers in the preparation of co-amorphous formulations. Int J Pharm 602. https://doi.org/10.1016/j.ijpharm.2021.120649

Yavarpour- Bali H, Pirzadeh M, Ghasemi-Kasman M (2019) Curcumin-loaded nanoparticles: a novel therapeutic strategy in treatment of central nervous system disorders. Int J Nanomed 14:4449–4460. https://doi.org/10.2147/IJN.S208332

Yildiz G, Aydoğmuş Z, Senkal F, Turan G (2019) Investigation of curcumin water solubility through emulsifying with biocompatible polyethylene glycol–based polymers. Food Anal Methods 12(10):2129–2138. https://doi.org/10.1007/s12161-019-01555-y